Journal of Magnetism and Magnetic Materials 322 (2010) 2571–2574

Contents lists available at ScienceDirect

Journal of Magnetism and Magnetic Materials

journal homepage: www.elsevier.com/locate/jmmm

Preferential crystallographic alignment in polycrystalline MnP

Ryan A. Booth [a], Melania Marinescu [b], JinFang Liu [b], Sara A. Majetich [a,*]

[a] Department of Physics, Carnegie Mellon University, Pittsburgh, 5000 Forbes Avenue, PA 15213, USA
[b] Electron Energy Corporation, Landisville, PA 17538, USA

ARTICLE INFO

Article history:
Received 23 November 2009
Received in revised form
16 February 2010
Available online 7 April 2010

Keywords:
Magnetocaloric effect
Manganese phosphide
Magnetocrystalline anisotropy
Texture

ABSTRACT

The existence of preferential crystallographic alignment in hot pressed and die upset manganese phosphide (MnP) was investigated using magnetic measurements and electron backscatter diffraction (EBSD). Pole figures calculated from the EBSD data show that die upsetting causes the ⟨1 1 0⟩ directions to align preferentially along the die upset (DU) direction with the ⟨0 0 1⟩ direction preferentially perpendicular to the DU direction. Magnetic measurements show that the die upsetting can reduce the saturation field relative to that of a similar sample with randomly oriented grains. Since the low-field magnetocaloric effect in single crystals of MnP has been shown to be greatest along the ⟨0 1 0⟩ direction and smallest along the ⟨1 0 0⟩ direction, this technique offers a means to achieve the advantages of single crystal alignment with the economy of using bulk processing techniques on polycrystalline material. The peak magnetic entropy change measured with the field applied along the DU direction in the DU sample was 3%, 5%, and 8% greater than the peak entropy change of a randomly oriented powder at fields of 2.0, 1.0, and 0.5 T, respectively.

1. Introduction

Since the discovery of the giant magnetocaloric effect in $Gd_5Si_2Ge_2$ [1], interest in magnetocaloric effect (MCE) materials has grown at an extraordinary pace due to the potential energy savings of MCE refrigeration devices. To date, most of this work has focused on the development of new materials systems, tuning the magnetic and structural transition temperatures, and reducing hysteretic losses, but in the last few years a number of significant studies have investigated the effect of microstructure on the magnetic and structural phase transitions. For instance, it was shown that the magnetocaloric effect increased by up to 80% in heat treated $Gd_5Si_2Ge_2$ relative to that of arc-melted $Gd_5Ge_2Si_2$ due to the redistribution of the Si and Ge atoms [2]. Lyubina et al. [3] showed that rapid solidification of $La(Fe,Si)_{13}$ alloys by melt spinning significantly reduced the annealing time necessary to remove α-Fe impurities while strongly reducing hysteresis. Trung et al. [4] showed that similar techniques could reduce hysteresis in the MnFe(P,Ge) materials. The use of micro analysis techniques such as transmission electron microscopy, scanning electron microscopy, and scanning Hall probe microscopy are also helping to elucidate the effect of microstructure on the characteristics and dynamics of phase transitions in MCE materials [5].

The most common figure of merit used to compare MCE materials is the magnetic entropy change per unit mass for a given change in magnetic field. For magnetic refrigeration to be a viable and energy efficient technology for small scale applications such as household air-conditioning and refrigeration, this magnetic field needs to be provided by permanent magnets, which are limited to a maximum strength of about 2 T. Because these materials are more easily saturated along certain crystallographic orientations, the MCE for low, fixed field changes is greatest along the easy-axis. For instance, the prototype room-temperature MCE material, gadolinium, saturates at ~0.8 T along the [0 0 0 1] direction and ~1.2 T along [10–10] [6]. Single crystal studies of $Gd_5(Si,Ge)_4$ have also shown that the magnetocrystalline anisotropy has a strong effect on the MCE [7]. Since very few MCE materials are cubic, crystallographic alignment techniques could be advantageous in many systems. In the past use of bulk processing techniques to achieve preferential crystallographic alignment combined with close attention to microstructure led to the successful development of high energy product permanent magnet materials like Ni–Fe–B and Sm–Co [8–10].

Single crystal studies of MnP have shown that strong magnetocrystalline anisotropy leads to a greater MCE along the easy axis [11,12]. MnP is an attractive system for this study of magnetic anisotropy because its rich magnetic phase diagram has inspired a significant body of single crystal work. The crystal structure of MnP is orthorhombic of space group *Pnma* with $a=0.5260$ nm, $b=0.3174$ nm, and $c=0.5919$ nm in the paramagnetic phase at 293 K, and $a=0.5241$ nm, $b=0.3181$ nm,

* Corresponding author. Tel.: +1 412 268 3105; fax: +1 412 681 0648.
E-mail address: sara@cmu.edu (S.A. Majetich).

0304-8853/$ - see front matter © 2010 Elsevier B.V. All rights reserved.
doi:10.1016/j.jmmm.2010.03.022

and $c=0.5903$ nm in the ferromagnetic phase at 60 K [13]. MnP undergoes a ferromagnetic to paramagnetic phase transition at a Curie temperature of 290 K [11]. In this paper we follow the $c>a>b$ convention for the lattice parameters. We examined the effect of hot pressing and die upsetting MnP. The texture of the processed samples was analyzed using electron backscatter diffraction (EBSD) to measure pole figures. The magnetocrystalline anisotropy was determined from magnetization curves, and the magnetic entropy change was calculated from isothermal magnetization curves using the Maxwell relation.

2. Experimental

MnP was prepared in a solid–vapor reaction by mixing Mn (99.999%, Aldrich) and P (99%, Aldrich) in a 3:1 Mn:P molar ratio, purging several times with high-purity argon, sealing the powder under vacuum of 10^{-2} torr in a borosilicate glass ampoule, and heating at 450 °C for 8 h. Phosphorus was added and this process was repeated with a 3:2 molar ratio, and finally a 3:3.15 molar ratio then heated for 3 days. The excess phosphorus was used to assure the correct final stoichiometry. This procedure circumvents the need for high temperatures and minimizes the amount of initial phosphorus present at any given time to decrease the fire and explosion hazards. The phase purity and lack of preferential crystallographic orientation was confirmed by X-ray diffraction. The preparation of the MnP single crystals used in this study was described previously [11].

The powder was further processed by hot pressing 3 g of powder under a vacuum of 10^{-6} torr. The pressing force was continuously increased to 2 tons and the temperature increased from 690 °C at the start of pressing to 740 °C at the end of pressing. A 0.64 g piece of the hot pressed sample was die upset with the pressure being continuously increased to 1 ton and the temperature being increased from 705 °C at the start of pressing to 785 °C at the end of pressing. In the die upset process a sample is deformed under pressure in an oversized die so that there is room for it to expand outward. This is different from hot pressing in which a powder is compressed to fill a die completely. The die upset deformation was calculated as the ratio of the ending height to the starting height and was found to be 70%. We define the die upset (DU) and hot pressed (HP) directions as the direction pressure applied during die upsetting or hot pressing processes.

A diamond saw was used to cut a $1\times1\times1$ mm^3 piece of both the die upset and hot pressed samples. Hysteresis loops of this sample were measured at 250 K with the magnetic field applied parallel and perpendicular to the DU and HP directions. The isothermal magnetization curves used to calculate the magnetic entropy change were measured with the field applied parallel to the DU direction. All magnetic measurements were performed using a Quantum Design SQUID magnetometer.

A second $2\times2\times10$ mm^3 sample was cut from the DU sample and the face perpendicular to the DU direction was mechanically polished. EBSD patterns were obtained from the polished face using an Oxford Instruments EBSD camera installed on a Phillips XL-30 scanning electron microscope (SEM). EBSD is a microanalysis technique used to create texture or phase maps of material surfaces. Alternatively, texture information could be obtained by analysis of peak height ratios in an X-ray diffraction 2θ scan [14] or from rocking curves or pole figures. Due to the existence of many overlapping peaks and lack of isolated *a*, *b*, or *c*-axis diffracting planes in the X-ray diffraction pattern, these more standard X-ray techniques could not be used on our sample. Orthorhombic materials are not typically studied for their texture, and previous neutron diffraction studies of orthorhombic uranium encountered similar difficulties [15]. In the uranium study mathematical modeling was employed to deconvolute the overlapping peaks. EBSD is a much simpler alternative.

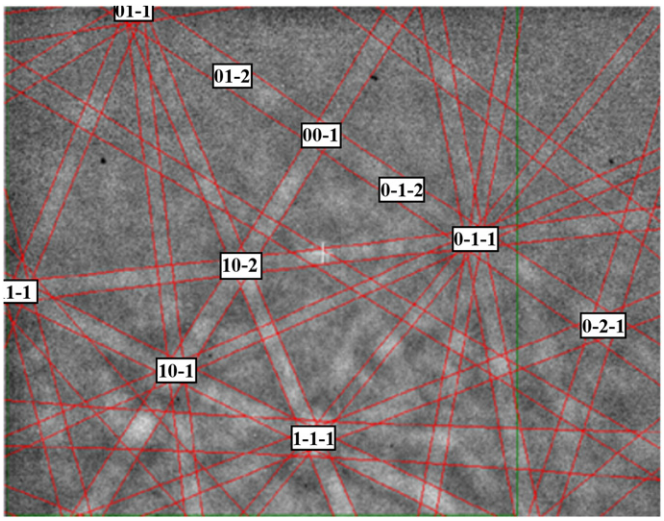

Fig. 1. A Kikuchi pattern from the polished die upset MnP sample with the Miller indices shown.

To create an EBSD pattern, the SEM electrons enter the sample and undergo multiple scattering processes as they typically do during the formation of a normal SEM image. As they exit, electrons diffract and form a Kikuchi pattern, which is recorded by the EBSD camera [16]. In typical X-ray and electron diffraction experiments with a single crystal or grain, the initial angle of the radiation interacting with the sample is defined and as a result diffraction spots are produced. In EBSD, the initial angle of a scattering process varies widely due to the multiple scattering events occurring within the sample and a Kikuchi pattern is formed instead of diffraction spots. The Kikuchi pattern contains information about the local crystallographic orientation, the local chemical phase, and local strain in a region of interest. Tango software (HLK) was used to index and analyze these patterns, an example of which is shown in Fig. 1.

Over a 240×22 μm^2 area 7277 sites of 0.5×0.5 μm^2 in size were sampled and indexed to obtain the local crystallographic orientation. The sampled area on the polished face of the die upset MnP is very close to the center of the original die upset piece. Pole figures were created from this information to analyze the texture of the sample.

3. Results and discussion

The percent difference in the magnetization when the magnetic field was applied parallel and perpendicular to the single crystal *b*-axis, DU, and HP directions is plotted in Fig. 2. From single crystal measurements, the *b*-axis is known to be the easy axis, the *a*-axis intermediate, and the *c*-axis the hard axis in MnP [17]. Therefore, the magnetic measurements do indicate that *b*-axis is preferentially oriented along the DU direction of the die upset sample, and to a much lesser degree the HP direction of the hot pressed sample.

Since single crystal measurements shown in Fig. 2 were made by first saturating the sample, then decreasing the field, the textured samples were measured in the same way. Also, the HP and DU samples have some degree of strain introduced by the hot pressing and die upsetting processes as indicated by an increase in the peak widths in the X-ray diffraction patterns compared to the peak widths of the powder pattern. Analysis of the peak

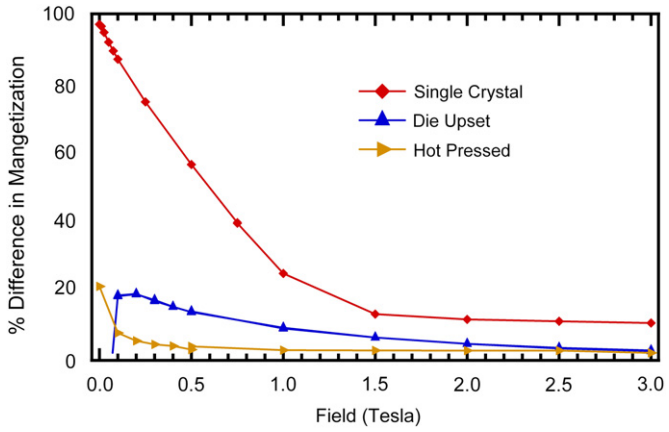

Fig. 2. Percent difference in magnetization between measurements with the field applied parallel and perpendicular to the *b*-axis, DU, and HP directions for the single crystal, die upset sample, and hot pressed samples, respectively.

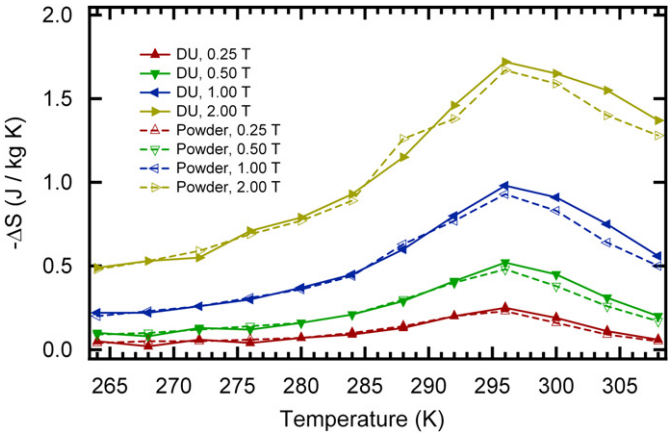

Fig. 3. Magnetic entropy change of the DU sample with the field applied parallel to the DU axis compared to the magnetic entropy change of a randomly oriented powder.

widths using the Scherrer relation gives average grain sizes of 55 nm in MnP powder and 20 nm in both the HP and DU samples. This suggests that strain is the source of hysteresis in the processed samples since it is not likely that the grains shrink during the deformation process. The measured hysteresis at 250 K was 440 Oe in the hot pressed sample and 300 Oe in the die upset sample. No measureable hysteresis was observed in the single crystals; thus the anomalously high difference in magnetization in the hot pressed sample and the negative difference in the die upset sample at zero field can be attributed to the history of the sample and a resulting non-zero remnant magnetization.

The difference in the magnetization between a field applied parallel to and perpendicular to the DU directions is 7.5% and 2.5% at 1.0 and 2.0 T, respectively. The difference in magnetization between a field applied parallel to the ⟨0 1 0⟩ direction (or parallel to the *b*-axis) and perpendicular to a combination of the ⟨1 0 0⟩ and ⟨0 0 1⟩ directions (or perpendicular to the *c*- and *a*-axes, respectively) was 24.9% and 10.2% at 1.0 and 2.0 T, respectively. The peak magnetic entropy change of the DU sample with the field applied parallel to the DU axis is about 3%, 5%, and 8% greater than the peak entropy change of a randomly oriented powder sample at fields of 2.0, 1.0, and 0.5 T, respectively as shown in Fig. 3.

The pole figures shown in Fig. 4 represent the distribution of the crystallographic directions ⟨1 0 0⟩, ⟨0 1 0⟩, ⟨0 0 1⟩, and ⟨1 1 0⟩ throughout the die upset sample. A pole figure is a stereographic projection of the distribution of a certain crystallographic direction in the real space of the sample [18]. For instance, a pole figure for the ⟨1 0 0⟩ family of directions in a cubic single crystal would have high intensity at the center, top, bottom, left, and right of the pole figure indicating the four-fold symmetry. In the die upset MnP sample, the ⟨1 1 0⟩ pole figure indicates that the ⟨1 1 0⟩ direction is strongly oriented along the die upset direction. While it is not immediately obvious why the ⟨1 1 0⟩ direction is the preferred packing direction for the die upset process, the texture is consistent with a deformation that only breaks symmetry in one direction. Texture that only breaks symmetry in one direction is referred to as fiber texture. The preference for the ⟨0 0 1⟩ direction to come out of the plane of the sample as indicated by the strong intensity in the center and horizontal band of the ⟨0 0 1⟩ pole figure is consistent with this fiber texture as the ⟨0 0 1⟩ direction is perpendicular to the ⟨1 1 0⟩ direction. The preference for the ⟨1 0 0⟩ and ⟨0 1 0⟩ directions to lie in the plane of the sample, as indicated by the concentration of intensity around the periphery of their respective pole figures, is also consistent with this fiber texture

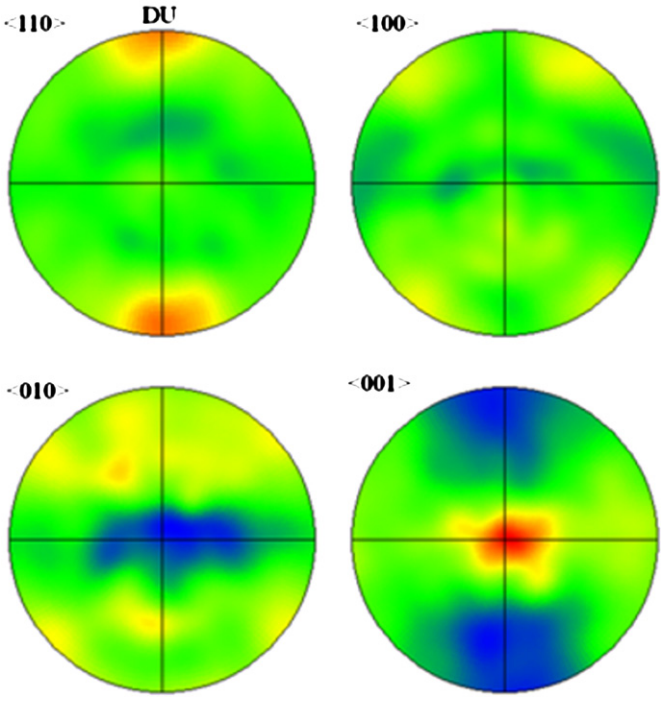

Fig. 4. Pole figures of the ⟨1 0 0⟩ or the *c*-axis, ⟨0 1 0⟩ or the *b*-axis, ⟨1 0 0⟩ or the *a*-axis, and ⟨1 1 0⟩ directions in MnP calculated from an EBSD map. The three axes: vertical, horizontal, and out of the plane are the same for each pole figure and refer to the sample coordinates. The vertical axis, DU, corresponds to the die upset direction. The axis pointing out of the page corresponds to the axis normal to the polished face of the sample. The lowest intensity is blue and the highest intensity is red. (For interpretation of the references to color in this figure the reader is referred to the web version of this article.)

since ⟨1 1 0⟩, ⟨1 0 0⟩, and ⟨0 1 0⟩ are mutually perpendicular to the ⟨0 0 1⟩ direction, which is preferentially out of the plane. The angular distribution of intensity along the DU direction in the ⟨1 0 0⟩ and ⟨0 1 0⟩ pole figures is also consistent with the fiber texture. Since the angle between the ⟨1 1 0⟩ and ⟨1 0 0⟩ directions is 33° and the angle between the ⟨1 1 0⟩ and ⟨0 1 0⟩ directions is 57°, it is expected that the ⟨0 1 0⟩ direction is more broadly distributed about the DU direction than the ⟨1 0 0⟩.

The preference for die upsetting to select the ⟨1 1 0⟩ direction in MnP is due to subtle physics of the structure and bonding

within the MnP crystal. These results show that it is not possible to give any stronger preference to the magnetically easy *b*-axis using the die upset technique under the temperature and pressure conditions described here. However, it may be possible to use a processing technique that breaks symmetry in two directions to strengthen the *b*-axis texture. One possible technique would be to die upset the sample in one direction, rotate 90° and die upset again. While cold rolling was shown not to be effective on MnP due to its brittleness, hot rolling could be. Because rolling selects two directions in a sample, the rolling direction and transverse direction, it is possible that rolling could also lead to stronger *b*-axis texture.

Although the EBSD and magnetic measurements qualitatively agree, it should be noted that the area sampled was in the middle of die upset sample and may not be representative of the texture throughout the sample as has been suggested in scanning X-ray diffraction experiments with Nd–Fe–B [10]. While EBSD only probes the surface of a material, probing regions closer to the edges could provide more information about distribution of the texture.

4. Conclusions

In conclusion, we have demonstrated that preferential alignment in polycrystalline samples of MnP can be achieved through die upset deformation and that the MCE of the textured sample is slightly greater than a randomly oriented sample. As most of the proposed MCE materials have some crystallographic and magnetic anisotropies, bulk processing techniques such as die upsetting should be investigated further as a means of achieving the advantage of single crystal properties with the economy of polycrystalline processing techniques. These effects could be particularly interesting in first-order transition materials as the coupling between the structural and magnetic transitions is much stronger than in second-order materials like MnP, and thus the physics of the magnetocaloric effect should depend more strongly on the texture of the sample.

Acknowledgements

This work was supported by Department of Energy under Grant no. DE-FG02-08ER46481.

References

[1] V.K. Pecharsky, K.A. Gschneidner, Phys. Rev. Lett. 78 (1997) 4494.
[2] A.O. Pecharsky, K.A. Gschneidner Jr., V.K. Pecharsky, J. Appl. Phys. 93 (2003) 4722.
[3] J. Lyubina, O. Gutfleisch, M.D. Kuz'min, M. Richter, J. Magn. Magn. Mater. 320 (2008) 2252.
[4] N.T. Trung, Z.Q. Ou, T.J. Gortenmulder, O. Tegus, K.H.J. Buschow, E. Brück, Appl. Phys. Lett. 94 (2009) 102513.
[5] J.D. Moore, K. Morrison, G.K. Perkins, D.L. Schlagel, T.A. Lograsso, K.A. Gschneidner Jr., V.K. Pecharsky, L.F. Cohen, Adv. Mater. 21 (2009) 3780.
[6] S. Yu., A.M. Dan'kov, V.K. Tishin, Pecharsky, K.A. Gschneidner Jr., Phys. Rev. B 57 (1998) 3478.
[7] M. Nazih, A. de Visser, L. Zhang, O. Tegus, E. Brück, Solid State Commun. 126 (2003) 255.
[8] A.M. Gabay, M. Marinescu, J.F. Liu, G.C. Hadjipanayis, J. Magn. Magn. Mater. 321 (2009).
[9] W. Grünberger, D. Hinz, A. Kirchner, K.H. Müller, L. Schultz, J. Alloys Compd. 257 (1997) 3318.
[10] L.H. Lewis, T.R. Thurston, V. Panchanathan, U. Wildgruber, D.O. Welch, J. Appl. Phys. 82 (1997) 3430.
[11] R.A. Booth, S.A. Majetich, J. Appl. Phys. 105 (2009) 07A926.
[12] M.S. Reis, R.M. Rubinger, N.A. Sobolev, M.A. Valente, K. Yamada, K. Sato, Y. Todate, A. Bouravleuv, P.J. Von Ranke, S. Gama, Phys. Rev. B 77 (2008) 104439.
[13] H. Fjellvag, A. Kjekshus, Acta Chem. Scand. A38 (1984) 563.
[14] D. Givord, A. Liénard, R. Perrier de la Bâthie, P. Tenaud et, T. Viadieu, J. Phys. Colloq. 46 (1985) C6-313.
[15] Y.C. Kim, H.J. Kim, C.H. Lee, B.S. Seong, S. Kim, Met. Mater. 4 (1998) 1101.
[16] F.J. Humphreys, J. Mater. Sci. 36 (2001) 3833.
[17] Y. Shapira, N.F. Oliveira Jr., C.C. Becerra, S. Foner, Phys. Rev. B 29 (1984) 361.
[18] J.S. Kallend, U.F. Kocks, A.D. Rollett, H.-R. Wenk, Mater. Sci. Eng. A 132 (1991) 1.